Lin and Bai, Aerosol and Air Quality Research, Vol. 6, No. 1, pp. 43-53, 2006

Temperature Effect on Pore Structure of Nanostructured Zeolite Particles Synthesized by Aerosol Spray Method

Yu-Chih Lin[1*] and Hsunling Bai[2]

[1.] Department of Environmental Engineering and Health,
Yuanpei Institute of Science and Technology, Hsinchu, Taiwan
306 Yuan-Pei Street, Hsin-Chu City 300, Taiwan
[2.] Institute of Environmental Engineering, National Chiao Tung University,

Abstract

This study investigated the effect of reaction temperature, ranging from 450 to 650 ^{o}C, on the pore structure of the nanostructured zeolite particles (NZP) synthesized by aerosol-assisted self-assembly (AASA). The results indicated that by using cetyltrimethylammonium bromide (CTAB) as a surfactant, the pore size distributions in the synthesized NZP from 450 to 550 ^{o}C were nearly uniform with geometric standard deviations of around 1.2. However, the uniformity is poorer at process temperature of 650 ^{o}C. A maximum surface area of 872 m^2/g could be reached at 550 ^{o}C with an average pore diameter of 2.0 nm, while a maximum pore diameter of 2.5 nm could be achieved at 450 ^{o}C with a surface area of 750 m^2/g. The results also indicated that a slight increase in the average pore diameter (d) of NZP from 2.0 to 2.5 nm led to an increase in the acetone adsorption capacity, even though its surface area was decreased; in which case (d=2.5 nm) the saturated adsorption of NZP was better than that of ZSM-5 zeolite.

Keywords: nano materials, porosity, tetraethoxysilane (TEOS), M41S, evaporation-induced interfacial self-assembly (EISA), aerosol pyrolysis, catalysis.

[*] Corresponding author. Tel: 886-3-5381183 ext. 8479; Fax: 886-3-6102337
E-*mail address*: yuchihlin@mail.yust.edu.tw

INTRODUCTION

Mesostructured materials of the M41S family have been synthesized (Kresge *et al*., 1992; Beck *et al*., 1992; Vartuli *et al*., 1994a; Beck *et al*., 1994; Vartuli *et al*., 1994b) and used as catalytic supports or VOCs adsorbents. They perform excellently because of their large surface area, controllable pore diameter, uniform pore size distribution, and hydrothermal as well as hydrophobic stability (Kawi and Te, 1998; Xia *et al*., 2001). The conventional hydrothermal method for manufacturing mesostructured materials is complex and time-consuming. Lu *et al*. (1999) developed the aerosol-assisted self-assembly (AASA) process for mesostructured silica nanoparticles, an aerosol pyrolysis method based on evaporation-induced interfacial self-assembly (EISA) method. The principle of AASA process is that the solvent evaporation of precursors, consisting of silica/surfactant/solvent, during aerosol procedure causes multi-phased assembly of surfactant micelle, which results in the inward mesostructure of silica droplet in a total synthesized time of several seconds. After the heating treatment, the surfactant was removed and the material appeared to be porous. Lu *et al*. showed that whether or not the silica particles exhibited mesostructures with the hexagonal, cubic or vesicular topologies was determined by the molar ratio of acidic tetraethoxysilane (TEOS) solution, the alcohol and the specific surfactants in the mixed precursors.

Applying the AASA process, Fan *et al*. (2001) synthesized mesoporous silica particles with hierarchically organized mesostructures and well-defined pore sizes templated by the surfactant, polystyrene spheres, and oil-in-water microemulsions. They found that the characteristics of mesostructure could be adjusted by the amounts and length scale of different templates.

Bore *et al*. (2003) reported the effect of synthesis parameters on the mesostructure of the silica particles utilizing TEOS precursor with the surfactant of cetyltrimethylammonium bromide (CTAB) as referred to Lu *et al*. (1999), but without adding alcohol into the precursors. They demonstrated that the ratio of surfactant to silica, and pH value of precursor influenced structural organization, pore size, and wall thickness. The effect of reactor temperature was investigated in the Bore *et al*. study, but only the extent of temperature effect on crystallinity.

Information on the temperature effect on the morphology of materials and physical properties of surface area and pore size distribution is limited in the literature. The surface area and pore size distribution as well as the morphology of the synthesized materials are important factors when they are to be applied as adsorbents or catalytic supports. Thus, this work uses TEOS, CTAB, hydrochloric acid (HCl), alcohol (EtOH) and deionized water as precursors, and studies the effect of reaction temperature of the chosen reagent on the physical characteristics of the nanostructured zeolite particles (NZP) synthesized by AASA process.

EXPERIMENTAL

Figure 1 depicts the experimental setup used in this study. A reagent bottle was placed in an ultrasonic oscillator with a thermal water bath at a temperature of 60 ^{o}C. For the AASA process in this study, the compositions of reagents are TEOS, CTAB, EtOH, H_2O and HCl. Besides, their molar ratios are 1, 0.1, 5, 20 and 0.004, individually. Under high pressure, a clean and dry airflow passed through an atomizer (TSI Model 3076) and drew the reagent from the bottle, yielding an aerosol flow rate of 2.5 LSTPmin^{-1}. The aerosol passed through a diffusion dryer to remove moisture, and flowed into a tube furnace with 50 cm of heating length. The temperatures of the tube furnace were adjusted at a 50 ^{o}C interval from 450 to 650 ^{o}C in the experimental tests to understand the temperature effect of the chosen reagent on the characteristics of the NZP synthesized by the AASA process. The total residence time of the reaction system ranges from six to eight seconds as the reaction temperature was varied in each experiment. The synthesized NZP were collected on a high-efficiency filter, and then placed in an oven to remove the surfactant at a temperature of 500 ^{o}C for five hours.

The average pore diameter and pore distribution were obtained using the Brunauer-Emmett-Teller (BET) equation by the Micromeritics ASAP2000 device after synthesis. The standard deviation of the repeated experiment was less than 3% in terms of the BET surface area, average and modal pore size. The other physical properties of the synthesized materials were analyzed by transmission electron microscopy (TEM, Philips TECNAI 20), powder x-ray diffraction (XRD, Rigaku D/MAX-B) and scanning electron microscopy (SEM, HITACHI-S4700).

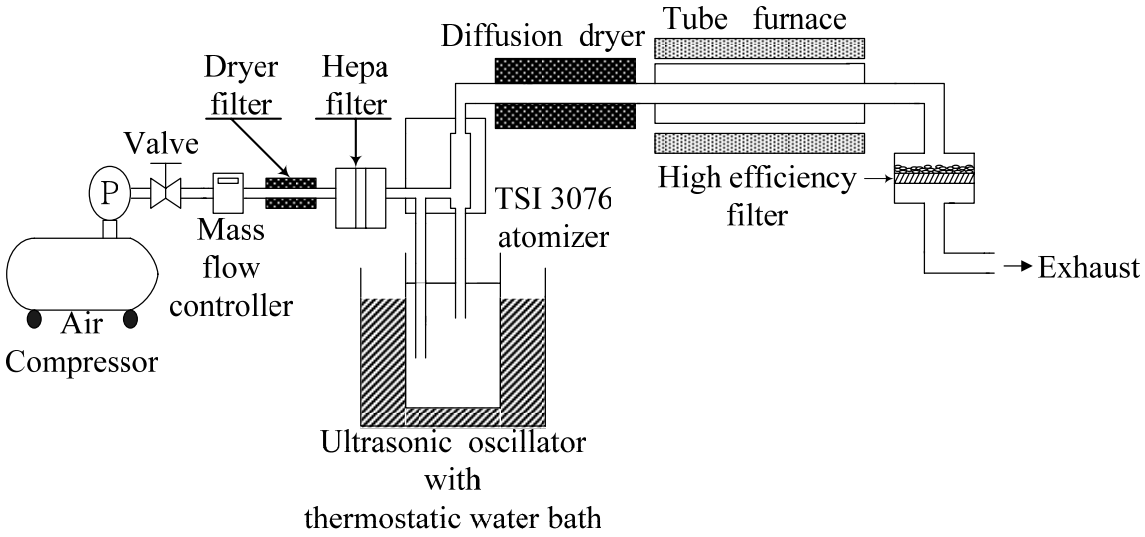

Figure 1. Experimental setup of AASA method to synthesize NZP.

Saturated adsorption of the NZP at different values of surface area and pore size was also tested, and the results were compared with that of the commercial ZSM-5 zeolite under the condition without moisture. Acetone was selected as the adsorbate which is one of the most common VOCs emitted from semiconductor industries. The adsorption temperature was 45 ^{o}C referring to the temperatures in practical VOCs adsorption operation of a zeolite concentrator in semiconductor industries.

A total of 0.3 ± 0.001 g of adsorbent was placed into the adsorption column (with inner diameter of 2.0 cm and height of 0.4 cm) under thermostat condition for each experiment. Thus the volume and the density of adsorption bed were 1.26 cm^3 and 0.24 g/cm^3, respectively. And the adsorbate residence time was 0.08 seconds as operated at an inlet flow-rate of 1000 cm^3/min in each adsorption experiment. The saturated adsorption of adsorbents were calculated by the breakthrough curves of the adsorbents, which were obtained by the acetone concentrations of process flow before and after the adsorption system were measured using GC/FID (China Gas Chromatograph 9800, Taiwan). The column used in the GC for analysis was Carbon Wax (2 m), and the temperatures of the injection point, FID, and oven were 100, 150, and 90 ^{o}C, respectively. The results shown in saturated adsorptions were the average data of three repeated experiments. The standard deviation of the repeated experiment was around 3% in terms of the acetone adsorption.

RESULTS AND DISCUSSION

Figure 2(a) illustrates the relationship between geometric standard deviation (σ_g) of pore diameter distribution, surface area and average pore diameter obtained at different operation temperatures. The geometric standard deviation (σ_g) of the pore diameter distribution was analyzed by the lognormal distribution. Each σ_g was calculated by the equation below (Hinds, 1999):

$$\ln \sigma_g = \left[\frac{\Sigma n_i (\ln d_i - \ln d_g)^2}{N-1} \right]^{1/2} \tag{1}$$

Where n_i was the pore volume in the group i, having a midpoint pore diameter d_i, among 1 and 6 nm and N was sum of n_i ($N = \Sigma n_i$). The d_g was the geometric mean of pore diameter defined as,

$$\ln d_g = \frac{\Sigma n_i \ln d_i}{N} \tag{2}$$

calculated for pore volumes having midpoint pore diameters between 1 and 6 nm.

One can see that if the reaction temperature was increased from 450 to 550 ^{o}C, the surface area of the NZP was increased from 750 to 872 m^2/g. The surface area reached maximum at a reaction temperature of 550 ^{o}C and then fell as the reaction temperature was further increased. The smallest surface area was 548 m^2/g, as synthesized at a reaction temperature of 650 ^{o}C. Raising the thermal energy from 450 to

550℃ was considered to contribute to an increase in the surface area of the NZP, given the compositions and ratios of reagents used. Thus, appropriate reaction temperatures promoted the micelles crystallization of surfactant due to self-organization and the encapsulation of silica on the micelles crystalline structure, which lead to a higher surface area.

The pure silica MCM-41 could be heated to 1,123K before structural collapse began (Chen *et al*., 1993; Kim *et al*., 1995). Therefore operating at the maximum reaction temperature, 650 ^{o}C, did not destroy the structural characteristics of the synthesized materials. The decrease in surface area at temperatures above 550 ^{o}C might be due to the possibility that higher temperatures led to the decomposition of some of the surfactant molecules in the aerosol flow before the AASA process; hence, fewer surfactant molecules were left to grow the structured micelle. It might be that higher temperatures led to the shrinkage due to initiation of sintering or thermal relaxation of the silica structure (Bore *et al*., 2003).

Figure 2(b) presents the distributions of pore diameter for NZP synthesized at different reaction temperatures. Based on the pore size distribution, one can calculate the mode pore diameters of 1.95 to 2.33 nm and the average pore diameters of 1.96 to 2.46 nm for operation temperature from 450 to 600 ^{o}C. The similar values of mode pore diameter and the average pore diameter in this temperature range indicate that the pore distributions are nearly uniform. The pore size distribution of NZP synthesized at 650 ^{o}C is broader as compared to the other process temperatures. This is also seen in Figure 2(b) by its related low pore volume, 2 cm^3/g, under mode pore size of 2.08 nm.

The uniformity of the synthesized NZP can be further demonstrated by values of geometric standard deviation (σ_g) of the pore diameter distribution. One can see from Figure 2(a) that the values of σ_g are small, ranging from around 1.18 to 1.24 for process temperatures from 450 to 600 ^{o}C. Under this circumstance one can say that the AASA process can produce near-monodispersed pore size. The uniformity of the pore-diameter distribution increases with increased surface area, with the smallest σ_g, 1.18, appearing at 550 ^{o}C and the largest, 1.30, appearing at 650 ^{o}C. It is estimated from the regression curve of the σ_g versus pore diameter that the largest pore diameter should be around 2.5 nm at σ_g of around 1.25. So one has to slightly compensate the pore size uniformity for achieving the largest pore diameter. Hence, from the pore diameter, pore uniformity and surface area point of view, an operation temperature range of 450 - 550 ^{o}C may be a good choice.

Figure 3 illustrated the TEM images of NZP synthesized at 550 ^{o}C. One can observe the mesopores with a wormlike structure distributed in the particles. The TEM images of materials synthesized at other temperatures are very similar in terms of their pore structures, hence they are not shown in this paper. The XRD spectra as shown in Figure 4 further indicated that synthesized NZP in the 450 - 650 ^{o}C temperature range is similar to hexagonal topologies, as indicated by the diffractive peak of (100) at $\theta = 2.4^{o}$ reflection as those of MCM-41 (Lu *et al*., 1999; Bore *et al*., 2003). The hexagonal pore

structure, instead of the wormlike morphology, can be improved by enhancing the ratio of CTAB/TEOS. (Bore *et al*., 2003)

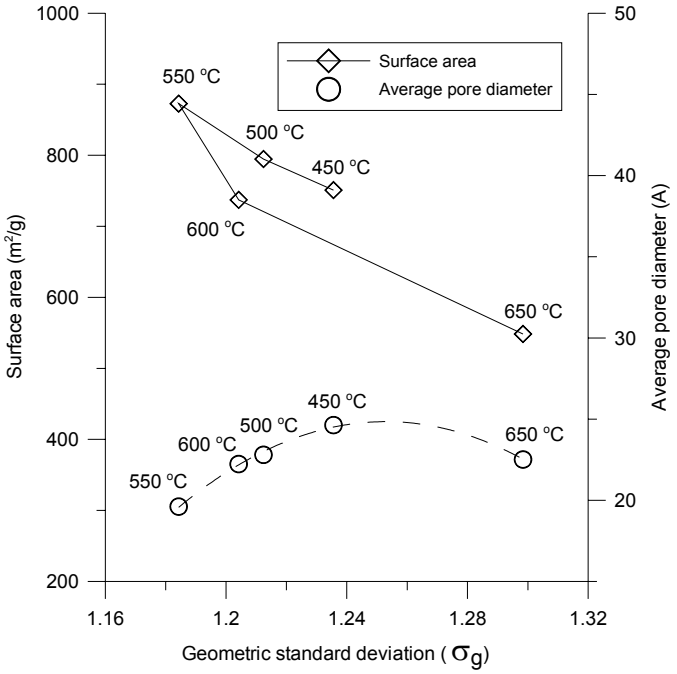

Figure 2(a). The inter-relationship between the geometric standard deviation of pore diameter distribution, the surface area, and the average pore diameter.

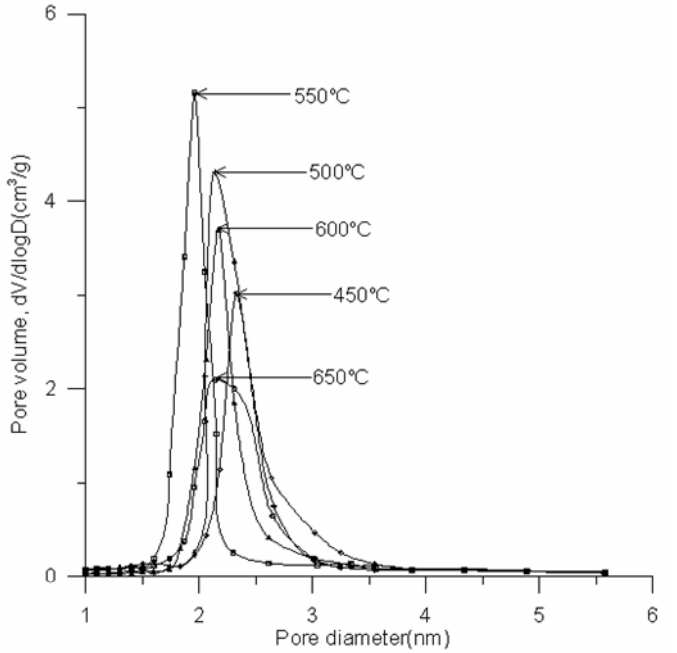

Figure 2(b). Effect of reaction temperature on the pore diameter distribution of synthesized NZP.

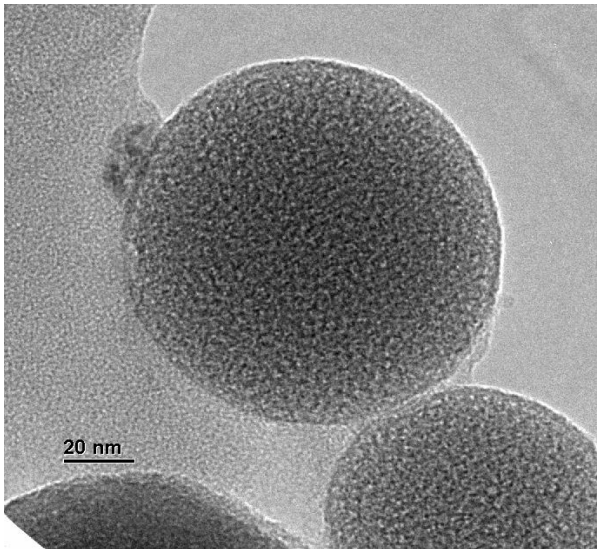

Figure 3. The TEM images of NZP synthesized at temperatures of 550 °C.

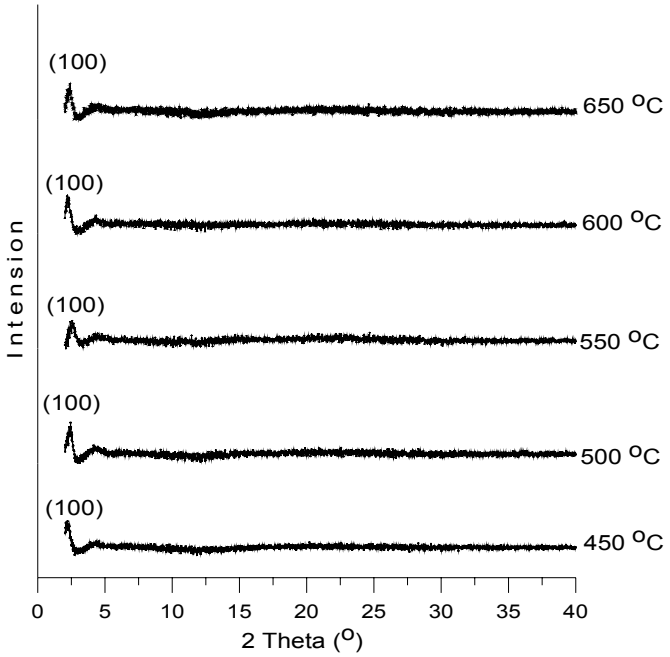

Figure 4. The XRD spectra of NZP synthesized at different temperatures.

Figure 5 shows the effect of reaction temperature on the distribution of particle size as observed by SEM micrographs. The exact particle size distribution can be measured by particle counter; however, the apparatus was unavailable and the standard deviation of the particle size distribution could not be calculated. But it was observed roughly, as Figure 5 shows, that the effect of temperature on the size distribution of particles was similar to that on the pore diameter uniformity. The synthesized particles

were more uniformly distributed at 550 °C, with particle size ranges from around 0.1 to 1.0 μm as illustrated by Figure 5(c). And it is relatively poly-dispersed for NZP synthesized at 650 °C, with particle size ranges from around 0.1 to 2.0 μm as illustrated by Figure 5(d).

Saturated adsorption of the NZP at different values of surface area and pore size was tested and the results were compared with that of the commercial ZSM-5 zeolite (Table 1). The average pore size was obtained from four multiples of surface area divided by total pore volume by BET model. The increase of pore size does not correspond to an increase of adsorption surface area. There was no significant difference between the total pore volume of each NZP. The BET surface area of NZP synthesized at 550 °C was 1.5 times that of ZSM-5 zeolite, but the saturated adsorption of NZP synthesized at 550 °C was 68.91 mg/g adsorbency; less than that of ZSM-5 zeolite at 73.25 mg/g adsorbency. Because the average pore diameter of NZP synthesized at 550 °C was 0.7 nm less than that of zeolite, there could be many tiny pore channels which are larger than nitrogen, but smaller than acetone, exiting in the synthesized NZP. The narrow pore channels of the NZP synthesized at 550 °C restrain adsorbing acetone and then cause a decrease in the saturated adsorption, even though NZP synthesized at 550 °C, owing the maximum surface area.

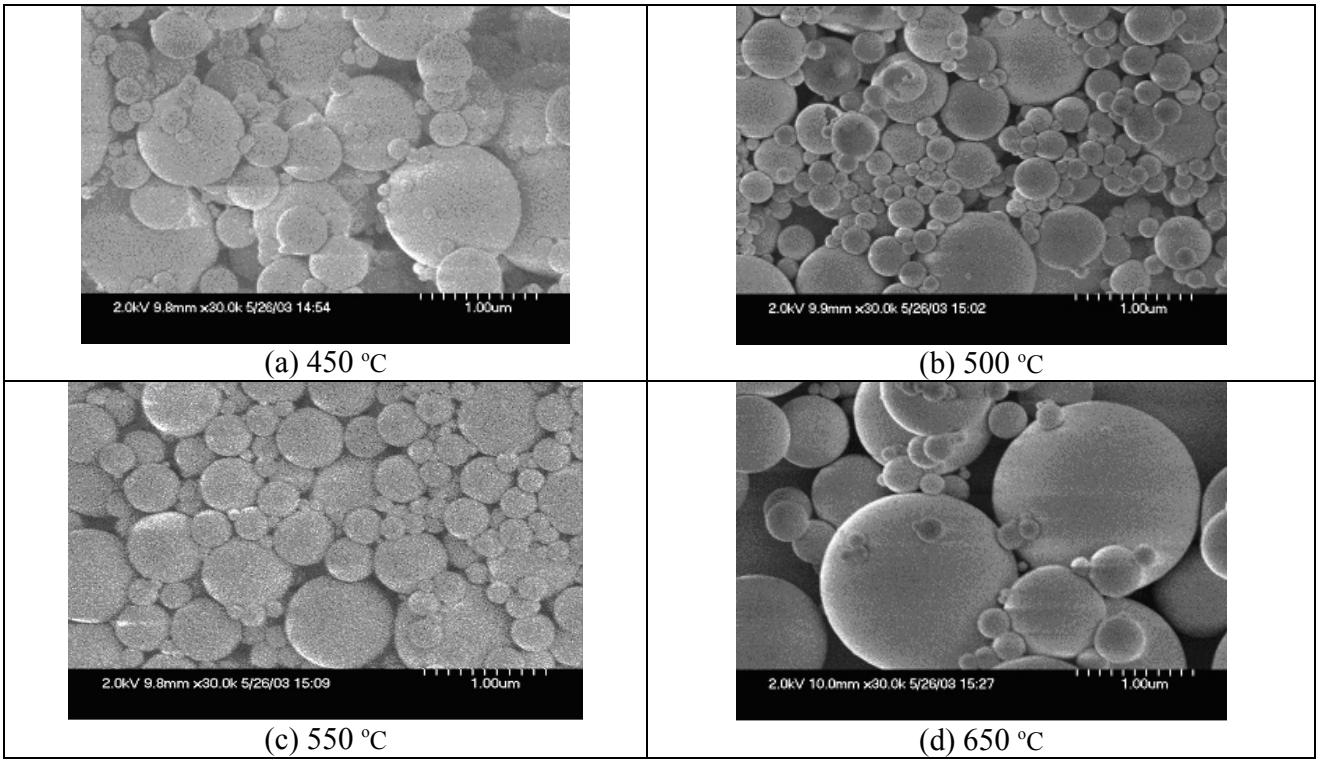

(a) 450 °C (b) 500 °C

(c) 550 °C (d) 650 °C

Figure 5. SEM images of NZP synthesized at different temperatures.

By altering the synthesized temperature from 550 to 450 °C, the average pore size of synthesized NZP was increased from 2.0 to 2.5 nm. But its surface area was slightly decreased from 872 to 750 m^2/g. As observed in Table 1, the NZP synthesized at 450 °C had better saturated adsorption, 82.53 mg/g adsorbency, than that of the commercial ZSM-5 zeolite. Thus, the saturated adsorption of the porous materials was affected by a slight increase in the pore size with a sacrifice in the surface area. Furthermore, the NZP show that they have better adsorption/desorption and hydrophobic characteristics as compared to the commercially available ZSM-5 zeolite (Lin *et al*., 2005).

Table 1. Saturated adsorption of NZP affected by the pore structure and compared with commercial ZSM-5 zeolite.

Adsorbents	Surface area(m^2/g)	Average pore size (nm)	Saturated adsorption of acetone (mg/g adsorbency)
NZP synthesized at 550 °C	872	2.0	68.91
NZP synthesized at 450 °C	750	2.5	82.53
ZSM-5 zeolite	356	2.7	73.25

CONCLUSION

This study applied the AASA process to synthesize nanostructured zeolite particles at various temperatures. The results indicate that the reaction temperature of the AASA process was a key parameter to determine the surface area, the average pore diameter, and the distributions of pore and particle size. Highly uniform pore size distribution in the synthesized materials could be achieved for temperatures ranging from 450 to 550 °C. A maximum pore size of 2.46 nm could be achieved at 450 °C, with a surface area of 750 m^2/g. At about 550 °C, maximum surface area (872 m^2/g) could be reached with the average pore size of 1.96 nm, and pore diameter distribution with the smallest geometric standard deviation appears to be the most uniform. In contrast, operational temperatures higher than 550 °C cause structural shrinkage of the NZP and decomposition of surfactant molecules in the synthesis.

The result of applying the NZP in the absorbent indicated that the adsorption capacity of synthesized NZP could be superior to that of the commercial zeolite, ZSM-5, due to its advantages of enhanced surface area and adjustable pore size. Future study can be done to optimize the surface area and the pore diameter distribution in terms of the practical application of the NZP as a gas adsorbent or catalytic support.

ACKNOWLEDGEMENT

The authors are grateful for the support from the National Science Council of the Republic of China under Contract No. NSC91-2211-E-009-011 and NSC92-2211-E-009-029.

REFERENCES

Beck J.S., Vartuli J.C., Kennedy G.J., Kresge C.T., Roth W.J. and Schramn S.E. (1994), Molecular or supramolecular templating: Defining the role of surfactant chemistry in the formation of microporous and mesoporous molecular-sieves. *Chem. Mater*. 6: 1816-1821.

Beck J.S., Vartuli J.C., Roth W.J., Leonowicz M.E., Kresge C.T., Schmitt K.D., Chu C.T.W., Olson D.H., Sheppard E.W., Mccullen S.B., Higgins J.B. and Schlenker J.L. (1992), A new family of mesoporous molecular sieves prepared with liquid crystal templates. *J. Am. Chem. Soc.* 114: 10834-10843.

Bore M.T., Rathod S.B., Ward T.L. and Datye A.K. (2003), Hexagonal mesostructure in powders produced by evaporation-induced self-assembly of aerosols from aqueous tetraethoxysilane solutions. *Langmuir* 19: 256-264.

Chen C.-Y., Li H.-X. and Davis M.E.(1993), Studies on mesoporous materials I. Synthesis and characterization of MCM-41. *Microporous Mater*. 2: 17-26.

Fan H.Y., Van Swol F., Lu Y.F. and Brinker C.J. (2001), Multiphased assembly of nanoporous silica particles. *J. Non-Cryst. Solids* 285: 71-78.

Hinds W.C.(1999), Aerosol technology: Properties, behavior, and measurement of airborne particles 2nd Edition, John Wiley & Sons, Inc., New York.

Kawi S. and Te M.(1998), MCM-48 supported chromium catalyst for trichloroethylene oxidation. *Catal. Today* 44: 101-109.

Kim J.M., Kwak J.H., Jun S. and Ryoo R. (1995), Ion-exchange and thermal-stability of MCM-41. *J. Phys. Chem.* 99: 16742-16747.

Kresge C.T., Leonowicz M.E., Roth W.J., Vartuli J.C. and Beck J.S. (1992), Ordered mesoporous molecular sieves synthesized by a liquid-crystal template mechanism. *Nature* 359: 710-712.

Lin Y.-C., Bai H.L. and Chang C.L.(2005), Applying hexagonal nanostructured zeolite particles for acetone removal. *J. Air & Waste Manage. Assoc.* 55: 834-840.

Lu Y., Fan H., Stump A., Ward T.L., Rieker T. and Brinker C.J. (1999), Aerosol-assisted self-assembly of mesostructured spherical nanoparticles. *Nature* 398: 223-226.

Vartuli J.C., Kresge C.T., Leonowicz M.E., Chu A.S., McCullen S.B.; Johnson I.D. and Sheppard E.W. (1994), Synthesis of mesoporous materials: Liquid-crystal templating versus intercalation of layered silicates. *Chem. Mater.* 6: 2070-2077.

Vartuli J.C., Schmitt K.D., Kresge C.T., Roth W.J., Leonowicz M.E., McCullen S.B., Hellring S.D., Beck J.S., Schlenker J.L., Olson D.H. and Sheppard E.W. (1994), Development of a formation mechanism for m41s materials. *Stud. Surf. Sci. Catal.* 84: 53-60.

Xia Q.-H., Hidajat K., and Kawi S. (2001), Adsorption and catalytic combustion of aromatics on platinum-supported MCM-41 materials. *Catal. Today* 68: 255-262.

Received for review, December 6, 2005
Accepted, February 21, 2006